Dalton Transactions

PAPER

View Article Online
View Journal

Cite this: DOI: 10.1039/c3dt53234h

Synthesis and characterisation of magnesium complexes containing sterically demanding *N,N′*-bis(aryl)amidinate ligands†

Graeme J. Moxey,*‡ Fabrizio Ortu, Leon Goldney Sidley, Helen N. Strandberg, Alexander J. Blake, William Lewis and Deborah L. Kays*

Received 15th November 2013,
Accepted 24th January 2014

DOI: 10.1039/c3dt53234h

www.rsc.org/dalton

Condensation reactions of carboxylic acids and anilines in the presence of polyphosphoric acid trimethylsilyl ester (PPSE) afforded a range of sterically demanding *N,N′*-bis(aryl)amidines, RN{C(R′)}N(H)R [R = Mes (Mes = 2,4,6-trimethylphenyl), R′ = Cy (Cy = cyclohexyl) $\mathbf{L^1}$H; R = Dipp (Dipp = 2,6-diisopropylphenyl), R′ = Cy $\mathbf{L^2}$H; R = Mes, R′ = Ph $\mathbf{L^3}$H; R = Dipp, R′ = Ph $\mathbf{L^4}$H; R = Mes, R′ = Dmp (Dmp = 3,5-dimethylphenyl) $\mathbf{L^5}$H; R = Dipp, R′ = Dmp $\mathbf{L^6}$H; R = Dmp, R′ = Cy $\mathbf{L^7}$H]. Amidines $\mathbf{L^1}$H–$\mathbf{L^7}$H have been characterised spectroscopically, and for $\mathbf{L^5}$H and $\mathbf{L^6}$H, by X-ray crystallography. Treatment of the amidines with di-*n*-butylmagnesium in THF solution afforded the monomeric magnesium bis(amidinates) [Mg($\mathbf{L^1}$)$_2$(THF)] **1**, [Mg($\mathbf{L^2}$)$_2$] **2**, [Mg($\mathbf{L^3}$)$_2$(THF)] **3**, [Mg($\mathbf{L^5}$)$_2$(THF)] **5**, [Mg($\mathbf{L^6}$)$_2$] **6**, [Mg($\mathbf{L^7}$)$_2$] **7**, and the magnesium mono(amidinate) complex [Mg($\mathbf{L^4}$)(^{n}Bu)] **4**. These complexes have been characterised spectroscopically, with **1–3**, **5** and **6** also being structurally authenticated. Comparison of the magnesium bis(amidinate) complexes reveals that the steric bulk of the amidinate ligand influences both the solid state structure and solution behaviour of these complexes.

Introduction

Amidinate ligands, [RN{C(R′)}NR]$^-$, are readily accessible and have been investigated in main group, transition metal and rare earth chemistry.[1–6] Amidinate ligands display a rich coordination chemistry, with both chelating and bridging coordination modes reported.[7] Metal amidinate complexes have found applications in many areas, including catalysis and materials science.[8] The steric and electronic properties of amidines can be readily tuned by changing the substituents at the nitrogen and carbon atoms of the ligand core, making amidinates an extremely versatile class of ligand, even more so than the ubiquitous cyclopentadienyls.[7] Studies have shown that as the steric bulk of the three substituents around the amidine backbone is increased, the NCN angle decreases, which consequently affects the coordination properties of the amidinate ligand. This in turn can influence the structure and reactivity of the resulting metal amidinate complex. This effect has been demonstrated elegantly by Jordan, using mono(amidinate) complexes of aluminium.[9,10] Changing the amidinate carbon substituent from Me to ^{t}Bu causes increased steric crowding around the Al centre, resulting in different synthetic outcomes when the two aluminium amidinate complexes were treated with B(C$_6$F$_5$)$_3$.[10]

In alkaline earth chemistry, bulky amidinate and the closely related guanidinate ligands have been used to stabilise complexes featuring hitherto unknown oxidation states and bonding modes, such as the Mg(I) species [LMg–MgL] (L = DippN{CN(^{i}Pr)$_2$}NDipp),[11] while less bulky amidinate ligands have been employed in magnesium chemistry for the synthesis of volatile complexes for MOCVD and ALD processes.[8,12] More recently, magnesium complexes containing amidinate supporting ligands have been shown to promote the dimerisation of benzaldehyde in the Tishchenko reaction.[13]

Despite the significant research interest in magnesium amidinates, only a handful of magnesium complexes containing *N,N′*-bis(aryl)amidinates have been structurally characterised.[14] Monomeric, homoleptic complexes were obtained using amidinate ligands with bulky substituents at the nitrogen and carbon atoms, despite the presence of coordinating solvents in the reactions: [Mg(ArN{C(R)}NAr)$_2$] [Ar = Dipp, R = *p*-Tol (*p*-Tol = 4-methylphenyl), Me].[15] The related [Mg(ArN{C(R)}NAr)$_2$]

School of Chemistry, University of Nottingham, University Park, Nottingham NG7 2RD, UK. E-mail: Deborah.Kays@nottingham.ac.uk; Fax: +44 (0)115-9513555; Tel: +44 (0)115-9513461

† Electronic supplementary information (ESI) available: Characterisation data for amidines $\mathbf{L^2}$H and $\mathbf{L^4}$H, the molecular structures of $\mathbf{L^5}$H and $\mathbf{L^6}$H, calculation of the Δ_{CN} parameter for **1–3**, **5**, **6**, $\mathbf{L^5}$H and $\mathbf{L^6}$H. CCDC 951585–951591. For ESI and crystallographic data in CIF or other electronic format see DOI: 10.1039/c3dt53234h

‡ Current address: Research School of Chemistry, Australian National University, Canberra, ACT 0200, Australia.

(Ar = Mes, R = ^{t}Bu), was prepared using hexane as the reaction medium.[16] When bulky substituents were only present at the nitrogen atoms (formamidinates), metallation reactions between di-*n*-butylmagnesium and formamidines yielded monomeric solvated magnesium complexes, *viz.* [Mg(ArN{C(H)}NAr)$_2$(solv)$_n$] [Ar = *p*-Tol, solv = THF, *n* = 2; solv = DME, *n* = 1; solv = TMEDA, *n* = 1] (DME = 1,2-dimethoxyethane, TMEDA = *N*,*N*,*N*′,*N*′-tetramethylethylenediamine).[17] These structures contrast the dinuclear species such as [Mg$_2$(^{i}PrN{C(Me)}N^{i}Pr)$_4$],[12] which are afforded when amidinate ligands containing less bulky substituents are used. The structures of these complexes demonstrate the interplay between ligand bulk, nuclearity and solvation in magnesium amidinates. A systematic study of the solution and solid state structures of magnesium bis(amidinates) is therefore imperative, given the renewed interest in alkaline earth chemistry[18,19] and requirement to develop structure–activity relationships for potential materials and catalysis applications.

Herein we report the synthesis of a range of new sterically demanding *N*,*N*′-bis(aryl)amidines from the condensation reactions of carboxylic acids and anilines in PPSE. We also report on a systematic investigation of the geometric ligand effects on the solution and solid state structures of magnesium complexes containing bulky *N*,*N*′-bis(aryl)amidinate ligands. These complexes complement the handful of structurally characterised magnesium bis(amidinate) complexes currently in the literature, facilitating a comprehensive view of magnesium bis(amidinate) chemistry.

Results and discussion

Synthesis

Synthesis of *N*,*N*′-bis(aryl)amidines. Treatment of a carboxylic acid with two equivalents of an aniline at 160 °C in PPSE (prepared *in situ* from hexamethyldisiloxane and phosphorus pentoxide in refluxing dichloromethane), followed by reaction work-up under basic conditions, afforded *N*,*N*′-bis(aryl)amidines **L^{1}H**–**L^{7}H** in good yields (Scheme 1). Amidines **L^{2}H** and **L^{4}H** have been previously prepared using a similar route.[20,21] The amidines **L^{1}H**–**L^{7}H** were characterised by ^{1}H and ^{13}C{^{1}H} NMR spectroscopy, infrared spectroscopy, mass spectrometry and elemental analysis. Amidines **L^{5}H** and **L^{6}H** have also been characterised by X-ray crystallography (see the ESI†).

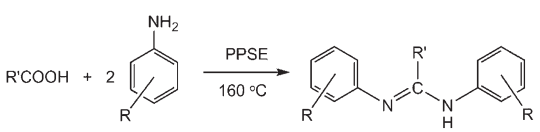

Scheme 1 Synthesis of *N*,*N*′-bis(aryl)amidines **L^{1}H**–**L^{7}H**. *Reaction and conditions*: PPSE, 160 °C, 16 hours. R = Mes, R′ = Cy **L^{1}H**; R = Dipp, R′ = Cy **L^{2}H**; R = Mes, R′ = Ph **L^{3}H**; R = Dipp, R′ = Ph **L^{4}H**; R = Mes, R′ = Dmp **L^{5}H**; R = Dipp, R′ = Dmp **L^{6}H**; R = Dmp, R′ = Cy **L^{7}H**.

This conceptually simple condensation route to amidines was first reported in 1984,[22,23] for amidines with substituents of low steric bulk, but has attracted little attention since.[20,24] There are two generally employed synthetic routes to symmetrical *N*,*N*′-bis(aryl)amidines;[25] (i) treatment of a lithium alkyl or aryl with a diarylcarbodiimide, which yields an intermediate lithium amidinate species and is subsequently quenched to form the amidine, and (ii) treatment of an acyl chloride with an amine affording the corresponding amide, which is then dehydrated to give an imidoyl chloride intermediate; subsequent reaction with an amine affords the amidine. The main disadvantage of these two routes is that each contains several synthetic steps, some involving the handling of air and moisture sensitive reagents. Furthermore, in route (i) the synthesis of diarylcarbodiimides typically involves the use of mercuric oxide,[26] and consequently the reaction work-up involves handling toxic mercury residues, and in route (ii) thionyl chloride is often used as the dehydrating agent.[27] The PPSE condensation route to amidines circumvents these issues and has comparable yields [**L^{4}H** has been previously prepared using route (ii), with a 60% yield].[21]

Synthesis of magnesium amidinate complexes. Amidines **L^{1}H**–**L^{7}H** react smoothly with di-*n*-butylmagnesium in THF, affording the monomeric magnesium bis(amidinate) complexes **1**–**3** and **5**–**7**, and the magnesium mono(amidinate) complex **4** (Scheme 2).

The isolation of a magnesium mono(amidinate) complex **4** was unexpected given that magnesium bis(amidinates) were obtained from analogous reactions employing closely related amidines. Attempts to isolate a magnesium bis(amidinate) complex by altering reaction conditions proved unsuccessful, consistently yielding **4**, and/or an intractable mixture of products. Magnesium mono(amidinate) complexes have been previously reported, such as [Mg(^{i}Pr)(DippN{C(^{t}Bu)}NDipp)(OEt$_2$)], prepared by treating ^{i}PrMgCl with [Li(DippN{C(^{t}Bu)}NDipp)] in diethyl ether.[28]

The influence of the steric bulk of the amidinate on the structure of the resulting magnesium complex is evident in comparing compounds **1**, **3** and **5** with **2** and **6**. The use of amidinate ligands featuring mesityl substituents on the nitrogen atoms yielded magnesium species which also featured a ligated THF molecule (**1**, **3** and **5**), whereas for complexes **2** and **6**, which contain amidinate ligands with bulkier Dipp

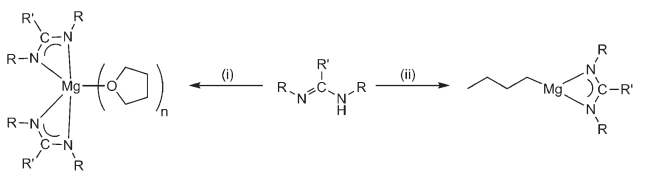

Scheme 2 Synthesis of complexes **1**–**7**. *Reaction and conditions*: (i) 0.5 ^{n}Bu$_2$Mg, THF, −78 °C → room temperature, − 2 ^{n}BuH. R = Mes, R′ = Cy, *n* = 1, **1**; R = Dipp, R′ = Cy, *n* = 0, **2**; R = Mes, R′ = Ph, *n* = 1, **3**; R = Mes, R′ = Dmp, *n* = 1, **5**; R = Dipp, R′ = Dmp, *n* = 0, **6**; R = Dmp, R′ = Cy, *n* = 0, **7**. (ii) ^{n}Bu$_2$Mg, THF, −78 °C → room temperature − ^{n}BuH. R = Dipp, R′ = Ph, **4**.

substituents, the homoleptic magnesium complexes were obtained. Homoleptic magnesium compounds containing all-nitrogen coordination spheres are of particular interest as precursors for magnesium-doped semiconductors.[12] Compounds **1–7** have been characterised by spectroscopy, elemental analysis, and in the case of compounds **1–3**, **5** and **6**, by single crystal X-ray crystallography.

Spectroscopic characterisation

Spectroscopic data for $\mathbf{L^2}$H and $\mathbf{L^4}$H are in good agreement with the reported data for these compounds.[20,21] The infrared spectra of the amidines $\mathbf{L^1}$H–$\mathbf{L^7}$H display an N–H stretching frequency at ~3350 cm^{-1} and C═N stretching frequencies in the region of 1610–1640 cm^{-1}. In the ^{1}H NMR spectra, the N–H resonance is in the region of 5.5 ppm, and in the $^{13}C\{^1H\}$ NMR spectra, the amidine backbone N*C*N resonance is in the region of 150–160 ppm; in good agreement with reported *N*,*N*′-bis(aryl)amidines.[20,21] Amidines often display several isomeric and tautomeric forms, due to C–N bond rotation and C═N isomerisation (E_{anti}, E_{syn}, Z_{anti}, Z_{syn}).[25] The presence of at least two isomers is evident in the ^{1}H and $^{13}C\{^1H\}$ NMR spectra of $\mathbf{L^1}$H–$\mathbf{L^7}$H, which is consistent with reported data for related amidines.[16,29,30]

The lack of a ν(N–H) absorption in the infrared spectra and the absence of a N–H resonance in the ^{1}H NMR spectra indicates complete deprotonation of the amidines in bulk vacuum dried samples of the isolated magnesium complexes **1–7**. Strong peaks in the infrared spectra in the region of 1640 cm^{-1} are attributed to ν(C–N) stretching bands. There is a downfield shift of the amidine backbone N*C*N resonance to 170–180 ppm in the $^{13}C\{^1H\}$ NMR spectra of these complexes compared to the free amidine values. In contrast to the amidines $\mathbf{L^1}$H–$\mathbf{L^7}$H, the NMR spectra of **1–7** indicate the presence of a single isomer, plausibly E_{anti}, which is consistent with the deprotonation and coordination of the amidine to a metal centre. The steric bulk of the nitrogen-bound substituents influence the behaviour of the magnesium amidinates in solution. The NMR spectra of **2** and **6** display four chemically inequivalent sets of isopropyl methyl groups and two isopropyl methine resonances, which can be attributed to extensive steric crowding around the magnesium centre, giving rise to two distinct 2,6-diisopropylphenyl environments. Similar solution behaviour has been reported for other magnesium complexes containing *N*,*N*′-bis(2,6-diisopropylphenyl)amidinate ligands.[15,28] In contrast, the NMR spectra of **1**, **3** and **5** display a single ligand environment, in agreement with the solution behaviour of $[Mg(ArN\{C(R)\}NAr)_2]$ (Ar = Mes, R = ^{t}Bu).[16]

Crystallographic characterisation

Crystalline samples of **1–3**, **5** and **6**, suitable for X-ray structure determinations, were grown from hexane, hexane–THF, or benzene-d_6 (see Experimental section), while crystals of $\mathbf{L^5}$H and $\mathbf{L^6}$H were grown from hexane–ethanol mixtures. Selected bond lengths and angles for complexes **1–3**, **5** and **6** are presented in Table 1, while Table 2 contains a summary of relevant crystal data and refinement parameters. The structures are depicted in Fig. 1–5. Selected bond lengths (Å) and angles (°) for $\mathbf{L^5}$H and $\mathbf{L^6}$H are presented in Fig. S1 and S2 in the ESI.†

In all complexes, the magnesium centre is bound to two chelating amidinate ligands; this coordination is supplemented by a ligated THF molecule in compounds **1**, **3** and **5**. Compounds **1**, **3** and **5** are five-coordinate monomers, with distorted square pyramidal geometry around the magnesium centre with the THF ligand occupying the apical position. In contrast, complexes **2** and **6** are four-coordinate monomers, with the magnesium centre adopting a distorted tetrahedral geometry. Broadly, the two N–C(backbone) distances in the amidinate ligands are the same, indicating ligand charge delocalisation over the amidinate NCN backbone (refer to the

Table 1 Selected bond lengths (Å) and angles (°) for compounds **1–3**, **5** and **6**

	1 C(*n*) = C(26)	**2** C(*n*) = C(32)	**3** C(*n*) = C(26)	**5** C(*n*) = C(28)	**6** C(*n*) = C(34)
Mg(1)–N(1)	2.2166(19)	2.0798(18)	2.1081(10)	2.1488(15)	2.059(3)
Mg(1)–N(2)	2.099(2)	2.0523(18)	2.1209(10)	2.0883(15)	2.050(3)
Mg(1)–N(3)	2.146(2)	2.0649(18)	2.1291(11)	2.0964(15)	2.045(3)
Mg(1)–N(4)	2.091(2)	2.0694(19)	2.1048(11)	2.1435(15)	2.067(3)
Mg(1)–O(1)	2.0832(17)		2.0568(9)	2.0626(13)	
N(1)–C(1)	1.326(3)	1.328(3)	1.3305(15)	1.331(2)	1.338(5)
N(2)–C(1)	1.342(3)	1.342(3)	1.3341(15)	1.338(2)	1.335(5)
N(3)–C(*n*)	1.329(3)	1.345(3)	1.3307(16)	1.336(2)	1.342(5)
N(4)–C(*n*)	1.350(3)	1.337(3)	1.3360(16)	1.335(2)	1.331(5)
N(1)–Mg(1)–N(2)	63.39(7)	65.04(7)	64.07(4)	63.71(5)	66.17(12)
N(1)–Mg(1)–N(3)	170.83(8)	126.28(8)	111.95(4)	109.42(6)	131.57(13)
N(1)–Mg(1)–N(4)	110.81(8)	154.46(8)	136.85(4)	166.56(6)	147.01(14)
N(2)–Mg(1)–N(3)	114.21(8)	141.96(8)	168.20(4)	129.58(6)	134.07(14)
N(2)–Mg(1)–N(4)	130.90(8)	122.12(8)	110.57(4)	110.65(6)	125.61(13)
N(3)–Mg(1)–N(4)	63.40(7)	65.45(7)	63.98(4)	63.80(5)	66.22(12)
N(1)–Mg(1)–O(1)	94.91(7)		111.06(4)	95.55(5)	
N(2)–Mg(1)–O(1)	114.63(8)		96.00(4)	115.08(6)	
N(3)–Mg(1)–O(1)	94.06(7)		95.78(4)	115.31(6)	
N(4)–Mg(1)–O(1)	114.45(7)		112.09(4)	97.87(6)	
N(1)–C(1)–N(2)	112.6(2)	112.60(18)	114.67(10)	113.88(14)	114.1(3)
N(3)–C(*n*)–N(4)	112.46(19)	112.90(17)	114.51(10)	114.06(14)	114.3(3)

Table 2 Crystallographic data for the X-ray structure determinations of **1**–**3**, **5**, **6**, L^5H and L^6H

	1·C_6D_6	**2**·C_6H_{14}	**3**·C_4H_8O	**5**·C_4H_8O	**6**·C_4H_8O	L^5H	L^6H
Formula	$C_{60}H_{74}D_6MgN_4O$	$C_{68}H_{104}MgN_4$	$C_{58}H_{70}MgN_4O_2$	$C_{62}H_{78}MgN_4O_2$	$C_{70}H_{94}MgN_4O$	$C_{27}H_{32}N_2$	$C_{33}H_{44}N_2$
FW	903.63	1001.86	879.49	935.59	1031.80	384.55	468.70
Space group	$P2_1/n$	$P2_1/c$	$P2_1/c$	$P2_1/n$	$P2_1/c$	$C2/c$	$P2_1/n$
a [Å]	12.3061(11)	12.3036(2)	12.57310(17)	16.6334(11)	18.2661(3)	27.7598(18)	11.5654(6)
b [Å]	21.499(2)	24.7484(4)	29.1302(4)	12.9516(9)	18.2865(2)	8.4639(3)	16.5227(8)
c [Å]	20.0063(18)	20.4769(4)	15.8661(2)	26.3010(18)	19.1208(2)	23.1109(15)	16.1572(9)
α [°]	90	90	90	90	90	90	90
β [°]	92.042(5)	95.9387(17)	112.1894(16)	101.876(7)	103.6657(13)	125.776(10)	109.525(3)
γ [°]	90	90	90	90	90	90	90
Vol [Å^3]	5289.8(8)	6201.64(19)	5380.72(12)	5544.7(6)	6206.02(14)	4405.4(4)	2910.0(3)
Z	4	4	4	4	4	8	4
D_{calc} [g cm^{-3}]	1.135	1.073	1.086	1.121	1.104	1.155	1.070
μ [mm^{-1}]	0.077	0.547	0.607	0.616	0.578	0.505	0.061
F(000)	1952	2208	1896	2024	2248	1664	1024
No. of indep. reflns (R_{int})	11 694 (0.0671)	12 380 (0.0434)	10 711 (0.0204)	11 162 (0.0447)	12 334 (0.0361)	4438 (0.0862)	3803 (0.0970)
R_1, wR_2 ($I > 2\sigma$)	0.0649, 0.1418	0.0723, 0.2013	0.0403, 0.1103	0.0522, 0.1376	0.0980, 0.2393	0.0826, 0.2253	0.0877, 0.1695

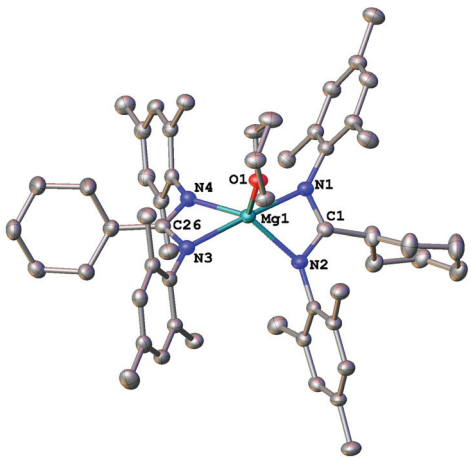

Fig. 1 Crystal structure of **1** with displacement ellipsoids set at 40% probability. Hydrogen atoms and the lattice benzene-d_6 molecule are omitted for clarity.

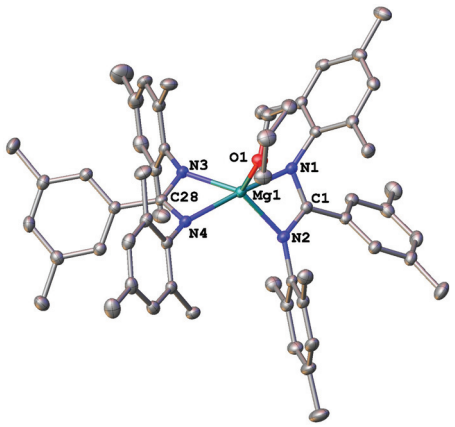

Fig. 3 Crystal structure of **5** with displacement ellipsoids set at 40% probability. Hydrogen atoms and the lattice THF molecule are omitted for clarity.

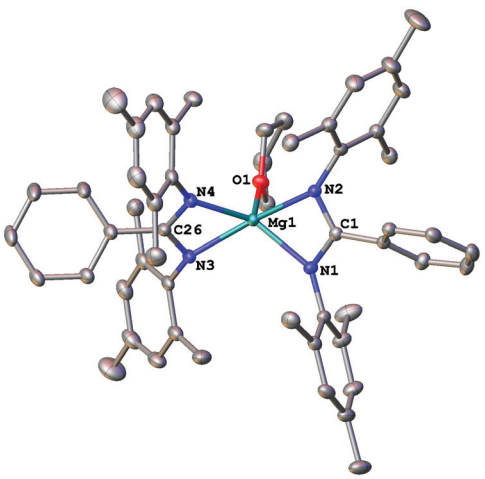

Fig. 2 Crystal structure of **3** with displacement ellipsoids set at 40% probability. Hydrogen atoms and the lattice THF molecule are omitted for clarity.

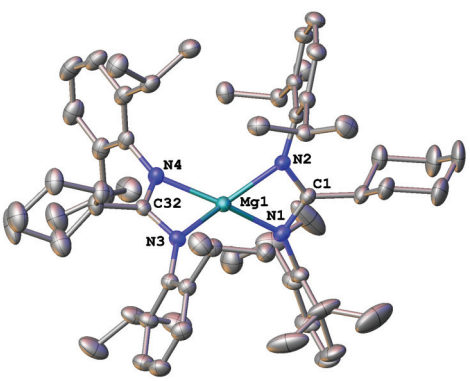

Fig. 4 Crystal structure of **2** with displacement ellipsoids set at 40% probability. Hydrogen atoms and the lattice hexane molecule are omitted for clarity.

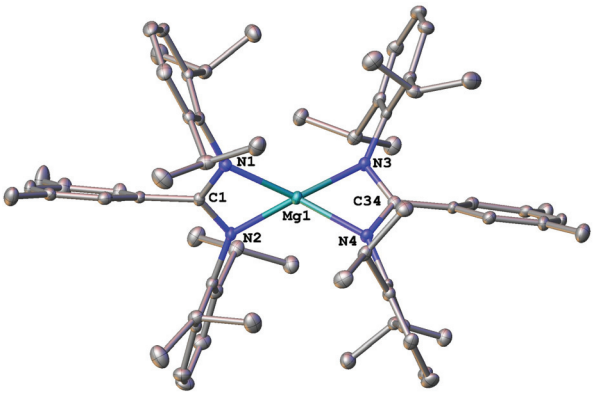

Fig. 5 Crystal structure of **6** with displacement ellipsoids set at 40% probability. Hydrogen atoms and the lattice THF molecule are omitted for clarity.

Δ_{CN} parameter calculations in the ESI†). The amidinate ligands adopt an E_{anti} arrangement on coordination to the magnesium centre, in contrast to the Z_{anti} and E_{syn} structures of $\mathbf{L}^5$H and $\mathbf{L}^6$H (ESI†).

Magnesium complexes of *N*,*N*′-bis(2,4,6-trimethylphenyl)-amidinate ligands. Due to the collective presence of mesityl substituents on the N atoms of the amidinate ligands in **1**, **3** and **5** (Fig. 1–3), the average Mg–N bond lengths in all three compounds are similar. The Mg–N bond distances range from 2.091(2)–2.2166(19) Å [average = 2.14(6) Å], in **1**, from 2.1048(11)–2.1291(11) Å [average = 2.116(11) Å] in **3**, and 2.0883(15)–2.1488(15) Å [average = 2.12(3) Å] in **5**. These average Mg–N bond lengths are in good agreement with the average Mg–N distances in the related five-coordinate magnesium amidinate [Mg(CyN{C(Ph)}NSiMe$_3$)$_2$(OEt$_2$)] (2.131 Å)[31a] and guanidinate [Mg{^{i}Pr$_2$NC(^{i}PrN)$_2$}$_2$(THF)] (2.124 Å).[31b]

The Mg–O(THF) distances [2.0832(17) Å for **1**, 2.0568(9) Å for **3** and 2.0626(13) Å for **5**] are shorter than the Mg–O(THF) bond distance in [Mg(^{i}Pr$_2$NC(^{i}PrN)$_2$)$_2$(THF)] (2.098(9) Å).[31] Although the steric bulk of the backbone C substituent on the amidinate (cyclohexyl in **1**, phenyl in **3**, 3,5-dimethylphenyl in **5**) has little effect on the average Mg–N bond lengths, it does influence the N–C–N angle. The bulky cyclohexyl backbone substituent in **1** results in more acute N–C–N angles [N(1)–C(1)–N(2) 112.6(2)°; N(3)–C(26)–N(4) 112.46(19)°] compared with the phenyl substituent in **3** [N(1)–C(1)–N(2) 114.67(10)°; N(3)–C(26)–N(4) 114.51(10)°] and the 3,5-dimethylphenyl substituent in **5** [N(1)–C(1)–N(2) 113.88(14)°; N(3)–C(28)–N(4) 114.06(14)°]. This trend is further exemplified in the structure of [Mg(MesN{C(^{t}Bu)}NMes)$_2$];[16] the bulky *tert*-butyl substituent on the amidine backbone gives rise to even more acute N–C–N angles of 109.0(3) and 110.2(3)°. The cyclohexyl backbone substituent in **1** (Fig. 1) is almost orthogonal to the NCNMg plane on each ligand [angle between cyclohexyl and N–Mg–N–C(backbone) least squares planes 93.45(7) and 87.40(7)°]. On moving to a less bulky substituent, these angles move away from orthogonality [54.54 and 44.22° in **3** (phenyl), 42.53(7) and 44.23(7)° in **5** (3.5-dimethylphenyl); Fig. 2 and 3].

Magnesium complexes of *N*,*N*′-bis(2,6-diisopropylphenyl)-amidinate ligands. The Mg–N distances in the four-coordinate compounds **2** and **6** (Fig. 4 and 5) range from 2.0523(18)–2.0798(18) Å [average = 2.067(11) Å] in **2**, and from 2.045(3)–2.067(3) Å [average = 2.055(10) Å] in **6**. These average values are in good agreement with the average Mg–N distances in the two crystallographically distinct molecules of [Mg(DippN{C(Me)}-NDipp)$_2$] (2.044 and 2.049 Å respectively),[28] as well as the average Mg–N distance in the amidinate compound [Mg(DippN{C(*p*-Tol)}NDipp)$_2$] (2.058 Å).[15] The N–C(backbone)–N angle of the amidinate ligands [112.60(18) and 112.90(17)° in **2**, and 114.1(3) and 114.3(3)° in **6**] are comparable with the analogous bite angles in **1** and **5** respectively, indicating that the steric bulk of the backbone C substituent of the amidinate ligand may have a greater influence on the ligand backbone N–C–N than the substituent on the N atoms of the amidinate, which is in agreement with Jordan's model.[9,10] In **2** and **6**, the two N–Mg–N–C(backbone) metallacycle planes are near orthogonal [angle between metallacycle least squares planes 61.65(9) in **2** and 76.58(16) in **6**], presumably to minimise steric repulsion between the 2,6-diisopropylphenyl substituents. This ligand arrangement accounts for the inequivalence of the isopropyl groups in the NMR spectra of **2** and **6**.

The influence of the amidinate C backbone substituent on the magnesium coordination environment is evident in comparing the *square planar* amidinate complex [Mg(DippN{C-(*p*-Tol)}NDipp)$_2$][15] with the distorted *tetrahedral* magnesium environment in the closely related amidinate compounds **2** and **6** (Fig. 4 and 5). The coplanar NCNMg metallacycles in the former compound were also attributed to preventing unfavourable interactions between diisopropylphenyl groups. Evidently, very small changes in the steric demands of the amidinate backbone C substituent can impart large structural variations. In a similar vein to **1**, the cyclohexyl backbone substituent in **2** is almost orthogonal to the N–Mg–N–C plane on each ligand [angle between cyclohexyl and N–Mg–N–C(backbone) least squares planes 96.96(11) and 85.45(11)°]. In **6**, the less bulky 3,5-dimethylphenyl backbone substituent gives rise to a non-orthogonal arrangement [54.79(15) and 46.69(14)° in **6**].

Conclusions

A range of bulky *N*,*N*′-bis(aryl)amidines was synthesised from the condensation reactions of carboxylic acids and anilines in the presence of PPSE, establishing the utility of this synthetic route to amidines of varying degrees of steric bulk. Treatment of the amidines with di-*n*-butylmagnesium in THF afforded mononuclear magnesium amidinates with concomitant formation of butane. The steric bulk of the amidinate ligand was found to influence both the solid state structure and solution behaviour of the magnesium amidinates. The effect of the amidinate ligand on the structure and properties of the resulting magnesium species is noteworthy, given the current

interest in magnesium amidinate complexes as catalysts and molecular precursors for MOCVD and ALD processes.

Experimental section

General remarks

All magnesium compounds prepared herein are air- and moisture-sensitive; therefore all reactions and manipulations were performed using standard Schlenk line and glove box equipment under an atmosphere of purified argon or dinitrogen. Hexane and pentane were dried by passing through a column of activated 4 Å molecular sieves. Dichloromethane was distilled over CaH_2. THF was pre-dried over Na wire and freshly distilled over sodium benzophenone ketyl under nitrogen. All solvents were degassed *in vacuo* and stored over a potassium mirror (hexane and pentane) or activated 3 Å molecular sieves (THF and dichloromethane) prior to use. Benzene-d_6 (Goss) was dried over potassium and THF-d_8 (Goss) was dried over CaH_2. Both were degassed with three freeze–pump–thaw cycles prior to use. ^{1}H and ^{13}C{^{1}H} NMR spectra were collected on Bruker AV 400, DPX 400 or DPX 300 spectrometers. Chemical shifts are quoted in ppm relative to TMS. Infrared spectra were recorded as Nujol mulls sandwiched between KBr plates on a Bruker Tensor 27 Fourier transform infrared spectrometer. Mass spectra were measured by the departmental service at the School of Chemistry, University of Nottingham. Elemental analyses were performed by Mr Stephen Boyer at London Metropolitan University. Amidines **L^2**H and **L^4**H have been previously prepared using a similar synthetic route,[20,21] and **L^4**H has also been prepared *via* reaction of *N*-(2,6-diisopropylphenyl)benzimidoyl chloride and 2,6-diisopropylaniline.[21,29,32] Di-*n*-butylmagnesium was obtained from Aldrich as a 1.0 M solution in heptane. The solvent was removed *in vacuo* and ^{n}Bu$_2$Mg was stored as a solid in the glove box. All other reagents were obtained from commercial sources and used as received. Yields refer to purified products and are not optimised.

General procedure for the synthesis of amidines L^{1}H–L^{7}H

The synthetic route is based on a modified literature procedure.[22,23] A Schlenk flask was charged with phosphorus pentoxide (4.5 g, 31.7 mmol), hexamethyldisiloxane (15.3 g, 20 mL, 94.1 mmol) and dichloromethane (20 mL). The reaction mixture was heated to reflux for 45 minutes under nitrogen, and then cooled to room temperature. All volatiles were removed *in vacuo*, affording a colourless, viscous syrup of PPSE, which was used *in situ* for the subsequent reaction. The PPSE was heated to 160 °C, and the relevant carboxylic acid (7.5 mmol) and aniline (15 mmol) were then added to the flask in quick succession under a flow of nitrogen. The condenser was replaced on the flask and the reaction maintained at 160 °C. After 16 hours, the reaction mixture was poured hot into a 1 M aqueous solution of NaOH, with vigorous stirring, affording an oily solid. The solid was extracted with dichloromethane (3 × 50 mL), the organic layer was separated and the aqueous phase was washed with dichloromethane (2 × 10 mL). The combined organic phases were dried over $MgSO_4$ and the solvent removed to yield the crude amidine. Crystallisation from hot hexane (**L^1**H, **L^2**H), or hexane–ethanol (**L^3**H–**L^7**H), afforded the pure amidines as colourless microcrystalline solids.

Data for MesN{C(Cy)}N(H)Mes (L^{1}H). From cyclohexanecarboxylic acid (0.96 g) and 2,4,6-trimethylaniline (2.03 g, 2.1 mL). Yield 1.81 g, 75%. ^{1}H NMR ($CDCl_3$, 298 K, 400 MHz): δ 1.05–1.39 (m, 4H, Cy–CH_2), 1.60–1.89 (m, 7H, Cy–CH_2 + Cy–C*H*N), 2.19 (s, 6H, CH_3), 2.23 (s, 6H, CH_3), 2.28 (s, 3H, CH_3), 2.29 (s, 3H, CH_3), 5.27 (s, 1H, N*H*), 6.87 (s, 2H, Ar*H*), 6.90 (s, 2H, Ar*H*). ^{13}C{^{1}H} NMR ($CDCl_3$, 298 K, 100 MHz): δ 17.8 (*C*H$_3$), 18.8 (*C*H$_3$), 20.7 (*C*H$_3$), 20.9 (*C*H$_3$), 25.8 (Cy–*C*H$_2$), 26.2 (Cy–*C*H$_2$), 31.2 (Cy–*C*H$_2$), 39.6 (Cy–H*C*N), 128.8 (Ar*C*H), 128.9 (Ar*C*H), 129.1 (Ar*C*H), 131.3 (Ar*C*), 133.7 (Ar*C*), 136.2 (Ar*C*), 136.5 (Ar*C*), 143.4 (Ar*C*), 160.3 (*C*N$_2$). Elemental analysis: calcd for $C_{25}H_{34}N_2$: C 82.82, H 9.45, N 7.73; found C 82.69, H 9.31, N 7.69. High res. mass spec. (ESI): calcd for $C_{25}H_{35}N_2$ [M + H]$^+$: 363.2795; measd 363.2804; calcd for $C_{25}H_{34}N_2Na$ [M + Na]$^+$: 385.2614; measd 385.2602. IR (Nujol): ν = 3339 (m, NH), 1642 (s, C═N), 1336 (w), 1270 (m), 1232 (m), 1212 (w), 1151 (w), 1032 (w), 852 (m), 802 (w) cm^{-1}.

Data for DippN{C(Cy)}N(H)Dipp (L^{2}H). From cyclohexanecarboxylic acid (0.96 g) and 2,6-diisopropylaniline (2.66 g, 2.83 mL). Yield 2.18 g, 65%. Spectroscopic and analytical data for **L^2**H are listed in the ESI† and are in agreement with previously reported data.[20]

Data for MesN{C(Ph)}N(H)Mes (L^{3}H). From benzoic acid (0.92 g) and 2,4,6-trimethylaniline (2.03 g, 2.1 mL). Yield 1.82 g, 68%. ^{1}H NMR ($CDCl_3$, 298 K, 400 MHz): δ 2.12 (s, 6H, CH_3), 2.20 (s, 3H, CH_3), 2.32 (s, 3H, CH_3), 2.35 (s, 6H, CH_3), 5.72 (s, 1H, N*H*), 6.74 (s, 2H, Ar*H*), 6.97 (s, 2H, Ar*H*), 7.21–7.32 (m, 3H, Ar*H*), 7.49–7.52 (m, 2H, Ar*H*). ^{13}C{^{1}H} NMR ($CDCl_3$, 298 K, 100 MHz): δ 18.0 (*C*H$_3$), 18.9 (*C*H$_3$), 20.7 (*C*H$_3$), 20.8 (*C*H$_3$), 127.2 (Ar*C*H), 128.2 (Ar*C*H), 128.8 (Ar*C*), 129.0 (Ar*C*H), 129.2 (Ar*C*H), 129.4 (Ar*C*H), 132.0 (Ar*C*), 134.5 (Ar*C*), 134.6 (Ar*C*), 135.5 (Ar*C*), 136.1 (Ar*C*), 143.3 (Ar*C*), 154.3 (*C*N$_2$). Elemental analysis: calcd for $C_{25}H_{28}N_2$: C 84.23, H 7.92, N 7.86; found C 84.11, H 8.05, N 7.72. High res. mass spec. (ESI): calcd for $C_{25}H_{29}N_2$ [M + H]$^+$: 357.2325; measd 357.2323. IR (Nujol): ν = 3358 (m, NH), 1632 (s, C═N), 1622 (s, C═N), 1495 (s), 1222 (w), 1212 (w), 1177 (w), 1093 (w), 1073 (w), 1028 (w), 892 (w), 852 (m), 808 (w), 768 (m), 698 (s) cm^{-1}.

Data for DippN{C(Ph)}N(H)Dipp (L^{4}H). From benzoic acid (0.92 g) and 2,6-diisopropylaniline (2.66 g, 2.83 mL). Yield 2.38 g, 72%. Spectroscopic and analytical data for **L^4**H are listed in the ESI† and are in agreement with previously reported data.[21]

Data for MesN{C(Dmp)}N(H)Mes (L^{5}H). From 3,5-dimethylbenzoic acid (1.13 g) and 2,4,6-trimethylaniline (2.03 g, 2.1 mL). Yield 2.02 g, 70%. ^{1}H NMR ($CDCl_3$, 298 K, 300 MHz): δ 2.14 (s, 6H, CH_3), 2.21 (s, 3H, CH_3), 2.22 (s, 6H, CH_3), 2.32 (s, 3H, CH_3), 2.36 (s, 6H, CH_3), 5.70 (s, 1H, N*H*), 6.74 (s, 2H, Ar*H*), 6.95 (s, 1H, Ar*H*), 6.97 (s, 2H, Ar*H*), 7.01 (s, 2H, Ar*H*). ^{13}C{^{1}H} NMR ($CDCl_3$, 298 K, 75 MHz): δ 18.0 (*C*H$_3$), 18.4 (*C*H$_3$), 19.0 (*C*H$_3$), 20.8 (*C*H$_3$), 21.3 (*C*H$_3$), 125.6 (Ar*C*H), 128.8 (Ar*C*H),

129.1 (ArCH), 131.0 (ArCH), 131.2 (ArC), 134.7 (ArC), 135.3 (ArC), 135.9 (ArC), 137.0 (ArC), 143.4 (ArC), 154.6 (CN_2). Elemental analysis: calcd for $C_{27}H_{32}N_2$: C 84.33, H 8.39, N 7.28; found C 84.22, H 8.49, N 7.17. High res. mass spec. (ESI): calcd for $C_{27}H_{33}N_2$ $[M + H]^+$: 385.2638; measd 385.2647; calcd for $C_{27}H_{32}N_2Na$ $[M + Na]^+$: 407.2458; measd 407.2466. IR (Nujol): ν = 3363 (w, NH), 1894 (w), 1621 (m, C=N), 1258 (m), 1209 (w), 1111 (m), 845 (w), 760 (m), 617 (w) cm^{-1}.

Data for DippN{C(Dmp)}N(H)Dipp (L^6H). From 3,5-dimethylbenzoic acid (1.13 g) and 2,6-diisopropylaniline (2.66 g, 2.83 mL). Yield 2.39 g, 68%. ^1H NMR ($CDCl_3$, 298 K, 300 MHz): δ 0.95 (d, 6H, CH(CH_3)$_2$, J = 6.9 Hz), 1.02 (d, 6H, CH(CH_3)$_2$, J = 6.6 Hz), 1.28 (d, 6H, CH(CH_3)$_2$, J = 6.6 Hz), 1.40 (d, 6H, CH(CH_3)$_2$, J = 6.9 Hz), 2.19 (s, 6H, CH_3), 3.23 (sept, 2H, CH(CH$_3$)$_2$, J = 6.6 Hz), 3.32 (sept, 2H, CH(CH$_3$)$_2$, J = 6.9 Hz), 5.68 (s, 1H, NH), 6.90 (s, 1H, ArH), 6.93–7.01 (m, 4H, ArH), 7.11–7.17 (m, 2H, ArH), 7.23–7.25 (m, 2H, ArH). $^{13}C\{^1H\}$ NMR ($CDCl_3$, 298 K, 75 MHz): δ 21.2 (CH(CH_3)$_2$), 22.4 (CH(CH_3)$_2$), 22.7 (CH_3), 24.5 (CH(CH_3)$_2$), 25.3 (CH(CH_3)$_2$), 28.3 (CH(CH$_3$)$_2$), 28.5 (CH(CH$_3$)$_2$), 123.2 (ArCH), 123.4 (ArCH), 123.5 (ArCH), 126.6 (ArCH), 127.4 (ArCH), 130.6 (ArCH), 134.0 (ArC), 134.7 (ArC), 137.0 (ArC), 139.5 (ArC), 143.7 (ArC), 145.4 (ArC), 154.3 (CN_2). Elemental analysis: calcd for $C_{33}H_{44}N_2$: C 84.56, H 9.46, N 5.98; found C 84.62, H 9.38, N 5.95. High res. mass spec. (ESI): calcd for $C_{33}H_{45}N_2$ $[M + H]^+$: 469.3577; measd 469.3588; calcd for $C_{33}H_{44}N_2Na$ $[M + Na]^+$: 491.3397; measd 491.3402. IR (Nujol): ν = 3443 (w), 3370 (w, NH), 1786 (w), 1761 (w), 1625 (s, C=N), 1599 (m), 1585 (m), 1355 (m), 1326 (w), 1257 (m), 1190 (w), 1176 (w), 1059 (m), 1042 (m), 949 (w), 934 (m), 858 (s), 827 (m), 796 (s), 762 (s), 751 (m), 723 (s), 687 (m), 478 (m) cm^{-1}.

Data for DmpN{C(Cy)}N(H)Dmp (L^7H). From cyclohexanecarboxylic acid (0.96 g) and 3,5-dimethylaniline (1.82 g, 1.87 mL). Yield 1.51 g, 60%. ^1H NMR (C_6D_6, 298 K, 400 MHz): δ 0.83–0.89 (m, 2H, Cy–CH$_2$), 1.05–1.07 (m, 2H, Cy–CH$_2$), 1.34–1.43 (m, 2H, Cy–CH$_2$), 1.70–1.79 (m, 2H, Cy–CH$_2$), 2.01–2.09 (m, 2H, Cy–CH$_2$), 2.20 (s, 12H, CH_3), 2.78–2.82 (m, 1H, Cy–CHN), 5.90 (br, 1H, NH), 6.59–6.66 (br, 4H, ArH), 7.57 (br, 2H, ArH). $^{13}C\{^1H\}$ NMR (C_6D_6, 298 K, 100 MHz): δ 21.4 (CH_3), 25.6 (Cy–CH$_2$), 25.8 (Cy–CH$_2$), 30.9 (Cy–CH$_2$), 31.3 (Cy–HCN), 117.4 (ArCH), 119.4 (ArCH), 123.6 (ArCH), 138.1 (ArC), 138.2 (ArC), 150.9 (CN_2). Elemental analysis: calcd for $C_{23}H_{30}N_2$: C 82.59, H 9.04, N 8.37; found C 82.48, H 8.85, N 8.25. High res. mass spec. (ESI): calcd for $C_{23}H_{31}N_2$ $[M + H]^+$: 335.2482; measd 335.2474; calcd for $C_{23}H_{30}N_2Na$ $[M + Na]^+$: 357.2301; measd 357.2299. IR (Nujol): ν = 3373 (s, NH), 1745 (w), 1714 (w), 1625 (s, C=N), 1613 (s, C=N), 1593 (s), 1320 (m), 1284 (w), 1270 (w), 1253 (w), 1172 (w), 1153 (s), 1031 (s), 970 (m), 947 (m), 908 (m), 837 (s), 755 (s), 715 (s), 685 (s), 591 (s) cm^{-1}.

General procedure for the synthesis of magnesium amidinates 1–7

A solution of di-*n*-butylmagnesium (0.2 g, 1.4 mmol) in THF (20 mL) was added dropwise to a solution of amidine (2.8 mmol) in THF (20 mL) at −78 °C with stirring. The reaction mixture was slowly warmed to room temperature and stirred overnight. Volatiles were removed *in vacuo* and the oily residue was extracted with hexane (**1**, **2**, **7**), or a hexane–THF mixture (**3**, **5**, **6**). The solution was filtered, concentrated to *ca.* 5 mL and cooled to −30 °C affording colourless crystals suitable for X-ray crystallography after several days. Crystals of **1** were also obtained from benzene-d_6. In the case of **4**, after removing the solvent, the residue was washed with pentane and dried to afford **4**.

Data for [Mg(L^1)$_2$(THF)] (1). From 1.05 g of L^1H. Yield 0.97 g, 82%. ^1H NMR (C_6D_6, 298 K, 300 MHz): δ 0.67–0.81 (m, 6H, Cy–CH$_2$), 1.20–1.31 (m, 2H, Cy–CH$_2$), 1.33–1.48 (m, 12H, Cy–CH$_2$ + THF–CH$_2$), 1.92–1.97 (m, 4H, Cy–CH$_2$), 2.33 (br s, 36H, CH_3), 2.45–2.60 (m, 2H, Cy–CHN), 3.73 (m, 4H, THF–OCH$_2$), 6.99 (s, 8H, ArH). $^{13}C\{^1H\}$ NMR (C_6D_6, 298 K, 75 MHz): δ 19.5 (CH_3), 20.8 (CH_3), 25.4 (THF–CH$_2$), 26.0 (Cy–CH$_2$), 27.8 (Cy–CH$_2$), 29.4 (Cy–CH$_2$), 43.2 (Cy–HCN), 68.9 (THF–OCH$_2$), 128.6 (ArCH), 130.9 (ArC), 132.6 (ArC), 145.3 (ArC), 177.3 (CN_2). Elemental analysis: calcd for $C_{54}H_{74}MgN_4O$: C 79.14, H 9.10, N 6.84; found C 79.06, H 9.01, N 6.88. IR (Nujol): ν = 1641 (w), 1608 (w), 1355 (m), 1311 (s), 1240 (s), 1209 (m), 1149 (m), 1007 (m), 879 (m), 851 (m), 831 (s), 686 (w), 526 (w), 460 (w) cm^{-1}.

Data for [Mg(L^2)$_2$] (2). From 1.29 g of L^2H. Yield 1.05 g, 80%. ^1H NMR (C_6D_6, 298 K, 300 MHz): δ 0.64 (d, 12H, CH(CH_3)$_2$, J = 6.6 Hz), 1.18–1.27 (m, 4H, Cy–CH$_2$), 1.33 (d, 12H, CH(CH_3)$_2$, J = 6.6 Hz), 1.31–1.49 (m, 8H, Cy–CH$_2$), 1.48 (d, 12H, CH(CH_3)$_2$, J = 6.7 Hz), 1.54 (d, 12H, CH(CH_3)$_2$, J = 6.5 Hz), 1.88–1.92 (m, 8H, Cy–CH$_2$), 2.45–2.58 (m, 2H, Cy–CHN), 3.43 (sept, 4H, CH(CH$_3$)$_2$, J = 6.8 Hz), 3.82 (sept, 4H, CH(CH$_3$)$_2$, J = 6.6 Hz), 7.09 (s, 2H, ArH), 7.12 (s, 2H, ArH), 7.20 (s, 2H, ArH), 7.22 (s, 2H, ArH), 7.23 (s, 2H, ArH), 7.25 (s, 2H, ArH). $^{13}C\{^1H\}$ NMR (C_6D_6, 298 K, 75 MHz): δ 22.9 (CH_3), 22.9 (CH_3), 23.5 (CH_3), 25.4 (CH_3), 25.7 (Cy–CH$_2$), 26.1 (Cy–CH$_2$), 26.2 (Cy–CH$_2$), 28.3 (CH(CH$_3$)$_2$), 28.4 (CH(CH$_3$)$_2$), 29.6 (Cy–CH$_2$), 30.0 (Cy–CH$_2$), 43.0 (Cy–HCN), 123.1 (ArCH), 123.2 (ArCH), 124.6 (ArCH), 142.7 (ArC), 143.1 (ArC), 143.5 (ArC), 180.6 (CN_2). Elemental analysis: calcd for $C_{62}H_{90}MgN_4$: C 81.32, H 9.91, N 6.12; found C 81.28, H 10.00, N 6.17. IR (Nujol): ν = 1918 (w), 1854 (w), 1794 (w), 1636 (s), 1586 (s), 1315 (m), 1258 (s), 1176 (w), 1099 (w), 1045 (w), 1021 (w), 970 (m), 933 (m), 876 (m), 802 (s), 784 (s), 769 (w), 748 (m), 723 (w), 696 (m), 578 (s), 528 (s), 481 (s), 451 (m) cm^{-1}.

Data for [Mg(L^3)$_2$(THF)] (3). From 1.03 g of L^3H. Yield 0.87 g, 75%. ^1H NMR (C_6D_6, 298 K, 300 MHz): δ 1.28 (m, 4H, THF–CH$_2$), 2.15 (s, 12H, CH_3), 2.20 (s, 24H, CH_3), 3.72 (m, 4H, THF–OCH$_2$), 6.65–6.73 (m, 6H, ArH), 6.75 (br s, 8H, ArH), 7.13 (m, 2H, ArH), 7.67–7.70 (m, 2H, ArH). $^{13}C\{^1H\}$ NMR ($CDCl_3$, 298 K, 75 MHz): δ 19.3 (CH_3), 20.7 (CH_3), 25.3 (THF–CH$_2$), 69.3 (THF–OCH$_2$), 126.8 (ArCH), 128.7 (ArCH), 128.9 (ArCH), 132.1 (ArCH), 132.0 (ArC), 134.7 (ArC), 135.9 (ArC), 145.0 (ArC), 172.8 (CN_2). Elemental analysis: calcd for $C_{54}H_{62}MgN_4O$: C 80.33, H 7.74, N 6.94; found C 80.02, H 7.72, N 6.84. IR (Nujol): ν = 1699 (m), 1302 (w), 1261 (s), 1215 (m), 1092 (s), 1027 (s), 852 (m), 800 (s), 766 (w), 696 (m) cm^{-1}.

Data for [Mg(L^4)(^{n}Bu)] (4). From 1.27 g of L^4H. Yield 0.33 g, 44%. ^1H NMR ($CDCl_3$, 298 K, 400 MHz): δ 0.66 (d, 6H, CH(CH_3)$_2$, J = 6.3 Hz), 0.79 (d, 6H, CH(CH_3)$_2$, J = 6.3 Hz), 0.87

(t, 3H, ^{n}Bu–CH_3, J = 7.1 Hz), 1.05–1.30 (m, 6H, ^{n}Bu–CH_2), 1.45 (d, 6H, CH(CH_3)$_2$, J = 6.1 Hz), 1.60 (d, 6H, CH(CH_3)$_2$, J = 6.3 Hz), 3.30 (m, 2H, CH(CH$_3$)$_2$), 3.95 (m, 2H, CH(CH$_3$)$_2$), 6.58–6.62 (m, 1H, ArH), 6.65–6.69 (t, 2H, ArH, J = 7.4 Hz), 6.80 (d, 2H, ArH, J = 7.3 Hz), 6.96–6.99 (t, 2H, ArH, J = 7.7 Hz), 7.11 (d, 2H, ArH, J = 7.3 Hz), 7.19 (d, 2H, ArH, J = 7.2 Hz). ^{13}C{^{1}H} NMR (CDCl$_3$, 298 K, 100 MHz): δ 22.5 (^{n}Bu–CH$_3$), 22.7 (CH(CH$_3$)$_2$), 23.2 (CH(CH$_3$)$_2$), 24.0 (CH(CH$_3$)$_2$), 25.2 (CH(CH$_3$)$_2$), 28.3 (CH(CH$_3$)$_2$), 28.9 (CH(CH$_3$)$_2$), 34.1 (^{n}Bu–CH$_2$), 34.2 (^{n}Bu–CH$_2$), 123.0 (ArCH), 123.3 (ArCH), 123.6 (ArCH), 124.4 (ArCH), 126.8 (ArCH), 129.0 (ArCH), 130.1 (ArCH), 131.9 (ArC), 142.2–142.5 (br, ArC), 142.8 (ArC), 176.3 (CN$_2$). Elemental analysis: calcd for $C_{35}H_{48}N_2Mg$: C 80.67, H 9.28, N 5.38; found C 80.50, H 9.11, N 5.22. IR (Nujol): ν = 1623 (s), 1578 (s), 1358 (m), 1318 (s), 1240 (s), 1185 (m), 1101 (s), 1055 (w), 1042 (w), 1027 (w), 964 (m), 934 (m), 918 (w), 802 (s), 785 (s), 767 (s), 697 (s), 522 (m) cm^{-1}.

Data for [Mg(L^5)$_2$(THF)] (5). From 1.11 g of L^{5}H. Yield 0.98 g, 79%. ^{1}H NMR (C_6D_6, 298 K, 300 MHz): δ 1.42 (m, 4H, THF–CH_2), 1.94 (s, 12H, CH_3), 2.27 (s, 12H, CH_3), 2.36 (s, 24H, CH_3), 3.84 (m, 4H, THF–OCH_2), 6.43 (s, 2H, ArH), 6.88 (s, 8H, ArH), 6.93 (s, 4H, ArH). ^{13}C{^{1}H} NMR (C_6D_6, 298 K, 75 MHz): δ 19.2 (CH$_3$), 20.7 (CH$_3$), 21.0 (CH$_3$), 25.4 (THF–CH$_2$), 69.2 (THF–OCH_2), 126.8 (ArCH), 128.6 (ArCH), 130.2 (ArC), 130.5 (ArCH), 132.2 (ArC), 135.6 (ArC), 136.0 (ArC), 145.3 (ArC), 173.2 (CN$_2$). Elemental analysis: calcd for $C_{58}H_{70}MgN_4O$: C 80.67, H 8.17, N 6.49; found C 80.57, H 8.25, N 6.41. IR (Nujol): ν = 2725 (w), 1759 (w), 1605 (m), 1307 (m), 1289 (w), 1261 (m), 1235 (m), 1212 (m), 1124 (w), 1068 (w), 1030 (s), 968 (m), 868 (s), 858 (s), 800 (s), 728 (s), 685 (s), 547 (m), 512 (s), 499 (m) cm^{-1}.

Data for [Mg(L^6)$_2$] (6). From 1.35 g of L^{6}H. Yield 1.05 g, 80%. ^{1}H NMR (C_4D_8O, 298 K, 300 MHz): δ 0.42 (d, 12H, CH(CH_3)$_2$, J = 6.5 Hz), 0.74 (d, 12H, CH(CH_3)$_2$, J = 6.6 Hz), 1.19 (d, 12H, CH(CH_3)$_2$, J = 6.8 Hz), 1.40 (d, 12H, CH(CH_3)$_2$, J = 6.5 Hz), 1.88 (s, 12H, CH_3), 3.20 (sept, 4H, CH(CH$_3$)$_2$, J = 6.8 Hz), 3.69 (sept, 4H, CH(CH$_3$)$_2$, J = 6.6 Hz), 6.46 (s, 2H, ArH), 6.56 (s, 4H, ArH), 6.65–6.71 (m, 4H, ArH), 6.78–6.84 (m, 4H, ArH), 6.95–6.98 (m, 4H, ArH). ^{13}C{^{1}H} NMR (C_4D_8O, 298 K, 75 MHz): δ 18.1 (CH_3), 20.5 (CH(CH$_3$)$_2$), 20.7 (CH(CH$_3$)$_2$), 21.7 (CH(CH$_3$)$_2$), 23.2 (CH(CH$_3$)$_2$), 25.9 (CH(CH$_3$)$_2$), 26.4 (CH(CH$_3$)$_2$), 120.7 (ArCH), 121.0 (ArCH), 121.6 (ArCH), 125.8 (ArCH), 126.6 (ArCH), 127.7 (ArC), 130.3 (ArC), 133.8 (ArC), 140.4 (ArC), 140.6 (ArC), 141.2 (ArC), 174.3 (CN$_2$). Elemental analysis: calcd for $C_{66}H_{86}MgN_4$: C 82.60, H 9.03, N 5.84; found C 82.69, H 9.11, N 5.73. IR (Nujol): ν = 1917 (w), 1855 (w), 1794 (w), 1636 (m), 1587 (m), 1579 (m), 1316 (m), 1269 (m), 1249 (w), 1214 (m), 1176 (m), 1158 (m), 1135 (m), 1103 (m), 1054 (m), 1045 (m), 1022 (m), 969 (s), 933 (m), 910 (w), 895 (w), 877 (w), 834 (m), 803 (s), 783 (s), 768 (s), 748 (s), 610 (w), 578 (s), 528 (s), 481 (s), 451 (s), 425 (s) cm^{-1}.

Data for [Mg(L^7)$_2$] (7). From 0.97 g of L^{7}H. Yield 0.48 g, 48%. ^{1}H NMR (C_6D_6, 298 K, 400 MHz): δ 0.84–0.89 (m, 4H, Cy–CH_2), 1.04–1.07 (m, 4H, Cy–CH_2), 1.34–1.48 (m, 4H, Cy–CH_2), 1.76–1.80 (m, 4H, Cy–CH_2), 2.00–2.13 (m, 4H, Cy–CH_2), 2.20 (br s, 24H, CH_3), 2.78–2.84 (m, 2H, Cy–CHN), 6.62–6.65 (br s, 8H, ArH), 7.57 (br s, 4H, ArH). ^{13}C{^{1}H} NMR (C_6D_6, 298 K, 75 MHz): δ 19.5 (CH_3), 20.8 (CH_3), 26.0 (Cy–CH$_2$), 27.8 (Cy–CH$_2$), 29.4 (Cy–CH$_2$), 43.2 (Cy–HCN), 128.6 (ArCH), 130.9 (ArC), 132.6 (ArC), 145.3 (ArC), 177.3 (CN$_2$). Elemental analysis: calcd for $C_{46}H_{58}MgN_4$: C 79.92, H 8.46, N 8.10; found C 79.83, H 8.38, N 8.03. IR (Nujol): ν = 2727 (w), 1625 (w), 1592 (s), 1311 (s), 1284 (w), 1260 (m), 1235 (s), 1153 (m), 1094 (s), 1023 (s), 885 (w), 842 (s), 800 (s), 699 (m), 686 (m), 604 (w) cm^{-1}.

X-ray structure determinations

Crystals of **1**·C_6D_6, **2**·C_6H_{14}, **3**·C_4H_8O, **5**·C_4H_8O, **6**·C_4H_8O, L^{5}H and L^{6}H were mounted on MicroMounts using YR-1800 perfluoropolyether oil (Lancaster) and cooled rapidly to 90 K in a stream of cold nitrogen using an Oxford Cryosystems low-temperature device. Diffraction data for **2**·C_6H_{14}, **3**·C_4H_8O, **5**·C_4H_8O, **6**·C_4H_8O and L^{5}H were collected on an Oxford Diffraction SuperNova Atlas CCD diffractometer equipped with a mirror-monochromated Cu-K$_\alpha$ radiation source (λ = 1.54184 Å), and for **1**·C_6D_6 and L^{6}H on a Bruker SMART APEX CCD diffractometer equipped with graphite-monochromated Mo-K$_\alpha$ radiation (λ = 0.71073 Å). Intensities were integrated from data recorded on 0.3° (APEX) or 1° (SuperNova) frames by ω rotation. Semiempirical absorption corrections based on symmetry-equivalent and repeat reflections (APEX) or Gaussian grid face-indexed absorption corrections with a beam profile correction (SuperNova) were applied. All non-H atoms were located using direct methods and difference Fourier syntheses. All non-H atoms were refined with anisotropic displacement parameters. Hydrogen atoms were constrained in calculated positions and refined with a riding model. Programs used were CrysAlisPro[33] and Bruker AXS SMART[34] (control), CrysAlisPro[33] and Bruker AXS SAINT[34] (integration), and SHELXS,[35] SHELXL[35] and OLEX2[36] (structure solution and refinement and molecular graphics). Crystal data for **1**·C_6D_6, **2**·C_6H_{14}, **3**·C_4H_8O, **5**·C_4H_8O, **6**·C_4H_8O, L^{5}H and L^{6}H can be found in Table 2. CCDC 951585–951591 (for **1**·C_6D_6, **2**·C_6H_{14}, **3**·C_4H_8O, **5**·C_4H_8O, **6**·C_4H_8O, L^{5}H and L^{6}H) contain the supplementary data for these compounds. *Variata*: For **1**, positional disorder was identified for atoms C(3) and C(5): the occupancies of the two components [C(3)–C(3A) and C(5)–C(5A)] were refined competitively, converging at a ratio of 0.795(5) : 0.205(5). Positional disorder was identified for atoms C(28) and C(30): the occupancies of the two components [C(28)–C(28A) and C(30)–C(30A)] were refined competitively, converging at a ratio of 0.885(5) : 0.115(5). Restraints were applied on the bond lengths of the cyclohexyl fragments C(27)–C(32) and C(2)–C(7). Sensible anisotropic parameters could not be refined for atoms C(5A), C(28A) and C(30A), so these were refined isotropically. For **2**, the anisotropic displacement parameters of atoms C(14)–C(16) and C(17)–C(19) were restrained. The unit cell of **2** contains four hexane molecules which have been treated as a diffuse contribution to the overall scattering without specific atom positions by PLATON SQUEEZE.[37] For **3**, hydrogens were placed in calculated positions and refined using a riding model. Methyl groups were refined as rigid rotors. Examination of the difference map showed that three methyl groups [C(23), C(40) and C(49)] had alternative possible positions for

the hydrogens. These were placed in calculated positions with 50 : 50 occupancy; the two positions were then allowed to refine as rigid rotors. Following this two further methyls were identified as split. These were placed in calculated positions; however refinement showed that a 75 : 25 occupancy split was more appropriate in this case. Again these groups were allowed to refine as rigid rotors. The unit cell of **3** contains four THF molecules which have been treated as a diffuse contribution to the overall scattering without specific atom positions by PLATON SQUEEZE.[37] For **6**, the anisotropic displacement parameters of atoms O(1) and C(67)–C(70) were restrained. For $\mathbf{L}^5$H, the NH hydrogen atoms on N(1) and N(2) were placed in calculated positions and are each half occupied, the result of two tautomers (Z_{anti} and E_{syn}) co-existing in the crystal. The N–H bond distances were restrained to be approximately equal. For $\mathbf{L}^6$H, the NH hydrogen was located from the difference map, and the N–H bond distance was restrained to 0.91 Å.

Acknowledgements

We thank the EPSRC (EP/G011850/1; PDRA GJM and for providing the funding for the X-ray diffraction equipment used herein) and the University of Nottingham for financial support of this work. We also thank Mr Stephen Boyer (Microanalysis Service, London Metropolitan University) for elemental analyses.

References

1 F. T. Edelmann, *Coord. Chem. Rev.*, 1994, **137**, 403.
2 J. Barker and M. Kilner, *Coord. Chem. Rev.*, 1994, **133**, 219.
3 P. J. Bailey and S. Pace, *Coord. Chem. Rev.*, 2001, **214**, 91.
4 F. T. Edelmann, *Chem. Soc. Rev.*, 2012, **41**, 7657.
5 J. A. R. Schmidt and J. Arnold, *J. Chem. Soc., Dalton Trans.*, 2002, 2890.
6 C. Jones, S. J. Bonyhady, N. Holzmann, G. Frenking and A. Stasch, *Inorg. Chem.*, 2011, **50**, 12315.
7 F. T. Edelmann, *Chem. Soc. Rev.*, 2009, **38**, 2253.
8 F. T. Edelmann, *Adv. Organomet. Chem.*, 2008, **57**, 183.
9 S. Dagorne, I. A. Guzei, M. P. Coles and R. F. Jordan, *J. Am. Chem. Soc.*, 2000, **122**, 274.
10 M. P. Coles, D. C. Swenson, R. F. Jordan and V. G. Young Jr., *Organometallics*, 1997, **16**, 5183.
11 S. P. Green, C. Jones and A. Stasch, *Science*, 2007, **318**, 1754.
12 A. R. Sadique, M. J. Heeg and C. H. Winter, *Inorg. Chem.*, 2001, **40**, 6349.
13 B. M. Day, W. Knowelden and M. P. Coles, *Dalton Trans.*, 2012, **41**, 10930.
14 Cambridge Structural Database version 5.34 (updates May 2013) was searched using ConQuest. F. H. Allen, *Acta Crystallogr., Sect. B: Struct. Sci.*, 2002, **58**, 380; I. J. Bruno, J. C. Cole, P. R. Edgington, M. Kessler, C. F. Macrae, P. McCabe, J. Pearson and R. Taylor, *Acta Crystallogr., Sect. B: Struct. Sci.*, 2002, **58**, 389.
15 R. T. Boeré, M. L. Cole and P. C. Junk, *New J. Chem.*, 2005, **29**, 128.
16 A. Xia, H. M. El-Kaderi, M. J. Heeg and C. H. Winter, *J. Organomet. Chem.*, 2003, **682**, 224.
17 M. L. Cole, D. J. Evans, P. C. Junk and L. M. Louis, *New J. Chem.*, 2002, **26**, 1015.
18 A. Torvisco, A. Y. O'Brien and K. Ruhlandt-Senge, *Coord. Chem. Rev.*, 2011, **255**, 1268.
19 W. D. Buchanan, D. G. Allis and K. Ruhlandt-Senge, *Chem. Commun.*, 2010, **46**, 4449.
20 Y. Luo, X. Wang, J. Chen, C. Luo, Y. Zhang and Y. Yao, *J. Organomet. Chem.*, 2009, **694**, 1289.
21 S. Bambirra, D. van Leusen, A. Meetsma and J. H. Teuben, *Chem. Commun.*, 2003, 522.
22 M. Kakimoto, S. Ogata, A. Mochizuki and Y. Imai, *Chem. Lett.*, 1984, **13**, 821.
23 S. Ogata, A. Mochizuki, M. Kakimoto and Y. Imai, *Bull. Chem. Soc. Jpn.*, 1986, **59**, 2171.
24 T. Elkin, S. Aharonovich, M. Botoshansky and M. S. Eisen, *Organometallics*, 2012, **31**, 7404.
25 M. P. Coles, *Dalton Trans.*, 2006, 985.
26 M. Findlater, N. J. Hill and A. H. Cowley, *Dalton Trans.*, 2008, 4419.
27 R. T. Boeré, V. Klassen and G. Wolmershausen, *J. Chem. Soc., Dalton Trans.*, 1998, 4147.
28 N. Nimitsiriwat, V. C. Gibson, E. L. Marshall, P. Takolpuckdee, A. K. Tomov, A. J. P. White, D. J. Williams, M. R. J. Elsegood and S. H. Dale, *Inorg. Chem.*, 2007, **46**, 9988.
29 C. A. Nijhuis, E. Jellema, T. J. J. Sciarone, A. Meetsma, P. H. M. Budzelaar and B. Hessen, *Eur. J. Inorg. Chem.*, 2005, 2089.
30 F. Qian, K. Liu and H. Ma, *Dalton Trans.*, 2010, **39**, 8071.
31 (*a*) M. Fan, Q. Yang, H. Tong, S. Yuan, B. Jia, D. Guo, M. Zhou and D. Liu, *RSC Adv.*, 2012, **2**, 6599; (*b*) B. Srinivas, C. Chang, C. Chen, M. Chiang, I. Chen, Y. Wang and G. Lee, *J. Chem. Soc., Dalton Trans.*, 1997, 957.
32 F. Liu, H. Gao, K. Song, Y. Zhao, J. Long, L. Zhang, F. Zhu and Q. Wu, *Polyhedron*, 2009, **28**, 673.
33 *CrysAlis PRO*, Agilent Technologies, Yarnton, England, 2010.
34 *SMART and SAINT*, Bruker AXS Inc., Madison, WI, 2001.
35 G. M. Sheldrick, *Acta Crystallogr., Sect. A: Found. Crystallogr.*, 2008, **64**, 112.
36 O. V. Dolomanov, L. J. Bourhis, R. J. Gildea, J. A. K. Howard and H. Puschmann, *J. Appl. Crystallogr.*, 2009, **42**, 339.
37 A. L. Spek, *J. Appl. Crystallogr.*, 2003, **36**, 7.